Effect of Ablation-Induced Roll Torques on Re-entry Vehicles

J. K. Kryvoruka* and T. T. Bramlette†
Sandia Laboratories, Livermore, Calif.

The results of a re-entry vehicle flight test program to evaluate the roll-producing effect of an ablating tape-wrapped carbon phenolic heat shield are presented. Included is a description of the thermal shield construction, which reveals the presence of small aerodynamic surfaces. Exposed by the ablation process during severe re-entry environment, these surfaces are capable of producing significant rolling moments. Instrumentation on-board the flight vehicle, designed to evaluate the aerodynamic and thermal response, indicated that the desired flight environment was achieved and that there was sufficient ablation to generate roll torque. A discussion of theoretical methods to predict the rolling moment coefficients is presented, as well as a comparison of the predicted coefficients with flight data. The vehicle was recovered intact, and the postflight inspection is described.

Nomenclature

p = roll rate, deg/sec or rad/sec
q = pitch rate, deg/sec
r = yaw rate, deg/sec
P_{crit} = vehicle natural pitch frequency, rad/sec
V = velocity, fps
M = Mach number
Q = dynamic pressure, lb/ft^2
H = mean sea-level altitude, ft
γ = flight path angle, deg
d = vehicle base diameter and reference length, ft
S = vehicle base area and reference area, ft^2, $S=\pi d^2/4$
I_x = vehicle roll moment of inertia, slug/ft^2
C_ℓ = total rolling moment coefficient, $C_\ell = \dot{p} I_x/QSd$
C_{ℓ_p} = roll damping moment coefficient, rad, $^{-1}C_{\ell_p} = \partial C_\ell / \partial(pd/2v)$
C_{M_α} = static stability coefficient, rad, $^{-1}$ $C_{M_\alpha} = \partial C_M/\partial\alpha$
α = vehicle total angle of attack, deg
C_{A0} = vehicle zero angle-of-attack axial force coefficient
$X_{c.p.}$ = aerodynamic center-of-pressure location, % length aft of nose
$X_{c.g.}$ = center-of-mass location, % length aft of nose
T = time, sec

Introduction

FLIGHT tests of full-scale re-entry vehicles with tape-wrapped carbon phenolic (TWCP) heat shields have, on many occasions, shown large excursions in spin rate.[1,2] These anomalous roll rate variations include spin-through-zero and the attainment of roll resonance, both of which can degrade system performance. Spin-through-zero can produce considerable impact dispersion,[3] whereas steady-roll resonance can result in excessive aerodynamic loading, as well as dispersion.[4,5] The cause of these spin rate excursions has been the subject of intensive study. Ablation phenomena have been given extensive treatment in the literature.[6-8] These studies have postulated surface irregularities caused by the aerodynamic flow pattern, which, in turn, lead to significant rolling moments. Observations made in ground test facilities have substantiated the development of patterns (including streamwise vortex grooving, turbulent wedge erosion, and cross-hatching) on conical wind-tunnel models made of camphor and naphthalene.

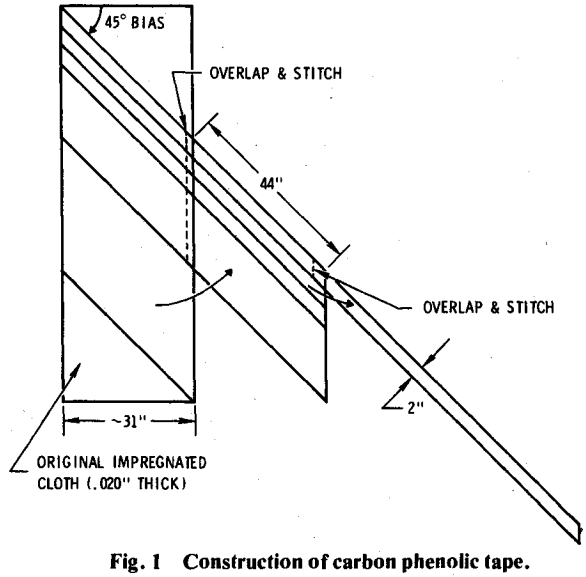

Fig. 1 Construction of carbon phenolic tape.

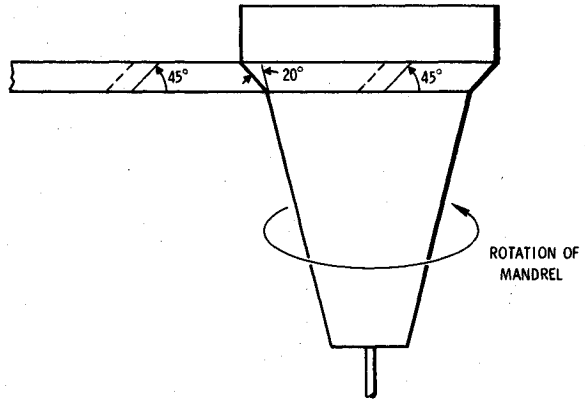

Fig. 2 Heat shield wrap method.

Presented at the AIAA 3rd Atmospheric Flight Mechanics Conference, Arlington, Texas, June 7-9, 1976 (in bound volume of Conference papers, no paper number) submitted June 28, 1976; revision received Dec. 20, 1976.

Index categories: LV/M Aerodynamics; LV/M Flight Testing; LV/M Aerodynamic Heating.

*Member of Technical Staff, Systems Development Department; present position—Program Manager, Litton Guidance & Control System Div., Woodland Hills, Calif. Member AIAA.

†Member of Technical Staff, Inorganic Materials Department.

It has been determined, however, that another source of rolling moments is dependent on the material of which the thermal shield is constructed, rather than on the aerodynamic flow pattern. Analysis of flight test data suggests a strong correlation between the direction of tape ends on TWCP heat shields and the vehicle spin rate performance. As shown by Larmour,[1] these seams or tape ends become exposed at or near boundary-layer transition for re-entry trajectories (or at the onset of significant aerodynamic heating and ablation) and, once exposed, act as small aerodynamic surfaces to produce significant roll torques and spin excursions. Several models for explaining the observed flight performance have been formulated. The application of these models to existing flight test data has been limited because of uncertainties in manufacturing process control on the vehicle tested, data acquisition, and alternate flight test objectives. In some cases it has not been possible to separate the roll torques that are purely heat-shield induced from those caused by other sources, such as trim-c.g. offset effects. In ground test facilities (wind tunnels) it is not possible to simulate a realistic flight environment, that is, one that is severe enough to produce ablation and mass blowing on the heat shield while providing the proper Mach and Reynolds numbers. Since heat shields have not been recovered intact, the character of the exposed aerodynamic surface is not known and remains a modeling uncertainty.

Tape-wrapped carbon phenolic heat shields have been given wide use in re-entry system application, because they provide excellent thermostructural properties at relatively low cost. However, owing to the ablation-induced roll torque phenomenon, system performance has been degraded severely. On the other hand, a thorough understanding of the phenomenon offers a means for passively controlling roll rate behavior, as discussed by Larmour.[9] It is important, therefore, that a theoretical understanding of this mechanism and its effect on flight performance be obtained and verified.

To assist in the development of this understanding, Sandia Laboratories initiated the Roll Torque Evaluation (RTE) program[10] designed to obtain accurate rolling moment data on an ablating TWCP heat shield in flight and to recover the thermal shield intact. The results of this test program are provided herein. A discussion of the re-entry vehicle thermal shield construction is presented, as well as a description of theoretical methods for estimating the heat shield roll torque.

Re-entry Vehicle Thermal Shield Construction

The heat shield was constructed to tape-wrapped carbon phenolic (CCA-2[1641] – 10 carbon cloth manufactured by Hitco) with a nominal thickness of 0.400 in. The steps used in manufacture of the tape are illustrated in Figs. 1 through 3. In this process, the material is made from phenolic-impregnated carbon cloth and cut on a 45-deg bias to maximize its stretch capability. The resulting trapezoidal sheets are overlapped and sewn together as illustrated, thus forming rolls which are approximately 40-yd long and 32-in. wide. These rolls have diagonal laps which run at an angle of 45 deg to the tape and appear every 44 in. (approximately). The rolls then are run through slitting machines to provide 2-in.-wide tapes. The tapes are wrapped aroung a conical mandrel (Fig. 2) to produce the 20-deg layup shown, thus causing the overlapping seams (tape joints) to have a 45-deg orientation relative to a longitudinal ray along the re-entry vehicle (RV) surface. The wrapped shield, illustrated schematically in Fig. 3, is cured and both inner and outer surfaces machined. In the curing process, the tape normally is compressed from 0.020-in. to approximately 0.014-in. thickness. The resulting outer surface is smooth, with the cavities shown in Fig. 3 filled in with phenolic. Aerodynamic heating produces phenolic removal, which exposes these aerodynamic surfaces and provides roll torque.

A positive wrap was employed over the aft 21.5 in. of the heat shields, whereas the forward 7.44 in. had a neutral wrap, which was accomplished by alternating positive and negative wraps in zones of approximately 2 in. in length. With this fabrication process, the total heat shield will produce a roll

Table 1 Flight vehicle physical properties

Cone half angle	7. deg
Bluntness ratio	0.223
Nose radius	1.06 in.
Base diameter, d	9.5 in.
Vehicle actual length	31.04 in.
Weight	89.74 lb
Center-of-mass distance, $x_{c.g.}$, from nose (53.5% of length)	16.783 in.
Pitch moment of inertia, I_Y	1.399 slug-ft^2
Yaw moment of inertia, I_Z	1.398 slug-ft^2
Roll moment of inertia, I_X	0.102 slug-ft^2
Static margin (at $M = 10$)	13% of length
Radial-c.g. offset	<0.001 in.

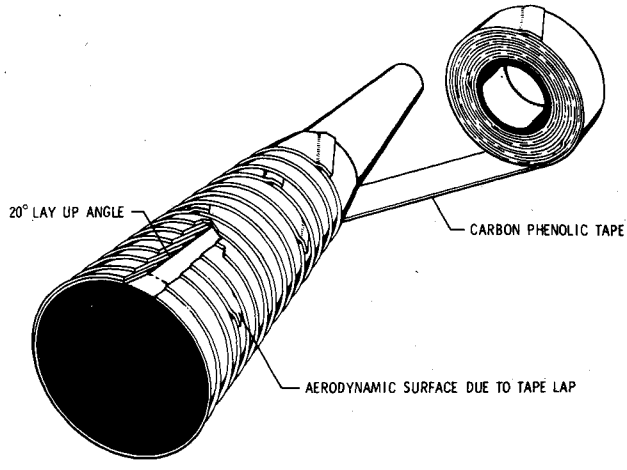

Fig. 3 Schematic of tape-wrapped carbon phenolic (TWCP) heat shield showing tape laps.

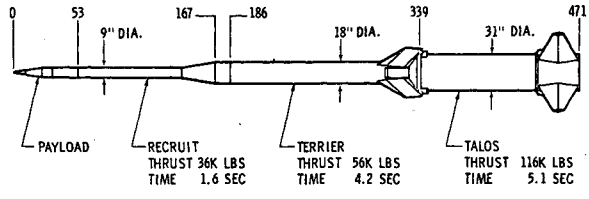

Fig. 4 TATER booster schematic.

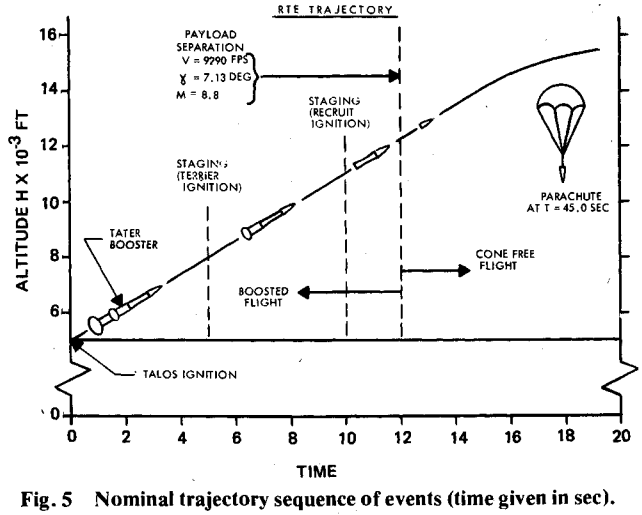

Fig. 5 Nominal trajectory sequence of events (time given in sec).

torque which causes the spin rate to increase in the positive direction (in a clockwise direction when viewed from the rear).

Flight System

Vehicle Design

A 7-deg cone with 22% bluntness ratio was selected as the test configuration. Other design parameters are given in Table 1. The heat shield manufacture was conducted under stringent process control to insure a meaningful test. Furthermore, the ratio of expected heat shield roll torques to extraneous torques (such as those due to trim-c.g. offset) was made very large so as to minimize measurement uncertainty. This was accomplished by designing in an unusually large static margin by re-entry system standards (13% static margin). Extremely close mass property control also was exercised so that lateral-c.g. offset was held to a minimum (less than 0.001 in). In addition, a low erosion graphite nose tip (Union Carbide ATJ-S graphite) was used to minimize trim angle development and its associated effect on roll torque.

A comprehensive instrumentation system was developed to measure the vehicle's aerothermodynamic and flight dynamic behavior.[10] Ablation was monitored through the use of specially designed thermal stacks placed at several locations in the heat shield. Each stack had three thermocouples imbedded at nominal depths of 0.020, 0.040, and 0.100 in. from the heat shield outer surface. These instruments provided a time history of the heat shield temperature profile. Burnout of the thermocouples was used to mark the progress of surface recession due to ablation. Accurate rate gyros and accelerometers were incorporated so that detailed flight behavior and aerodynamic characteristics could be obtained.

The payload was equipped with a parachute recovery system for soft landing. Intact recovery of the flight vehicle thus has afforded a close postflight investigation of the ablated heat shield and nosetip.

Boost System

A Talos-Terrier-Recruit (TATER) three-stage rocket system shown in Fig. 4 was chosen, since it provided a unique and inexpensive system capable of producing a severe aerothermodynamic environment. The booster system[11] produces realistic flight environments in terms of the desired Mach number, Reynolds number, and heating/ablation rates that are necessary to investigate the roll torque effect.

Flight Test Data

Trajectory

The nominal trajectory profile showing three boost stages, free flight of the payload, and parachute recovery is depicted in Fig. 5. Reconstruction of the trajectory from radar, cinetheodolite, and onboard instrumentation produced the payload separation conditions given in Table 2 and the payload free flight characteristics shown in Fig. 6. Maximum conditions, which occurred prior to separation, were 75 atm and approximately 2500 Btu/ft^2-sec nosetip stagnation pressure and heating rate, respectively. Peak cone surface heating (near the base) was 600 Btu/ft^2-sec.

Motion Data

The components of body angular rate (pitch, yaw, and roll rates), as determined from the onboard rate gyro, are given in

Table 2 Payload separation conditions

Velocity	9710 fps
Mach number	8.8
Flight-path angle	4.25 deg
Altitude (MSL)	10,525 ft
Dynamic pressure	77,600 lb/ft^2
Roll rate	−3500 deg/sec
Time of separation	13.0 sec

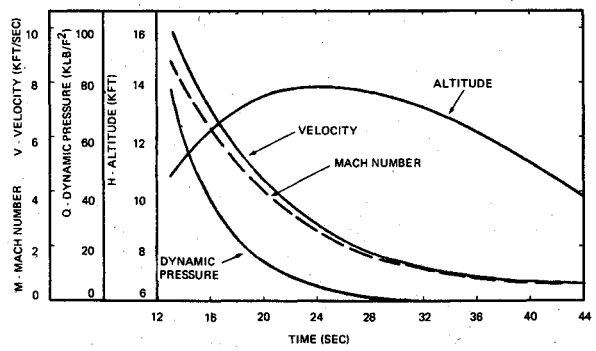

Fig. 6 Flight Mach number, velocity, dynamic pressure, and altitude history.

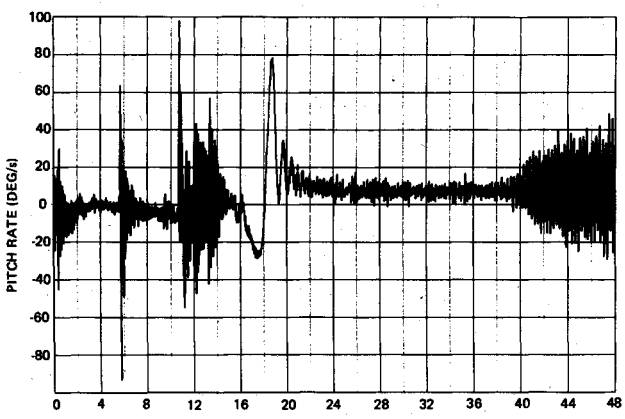

a) Pitching velocity history

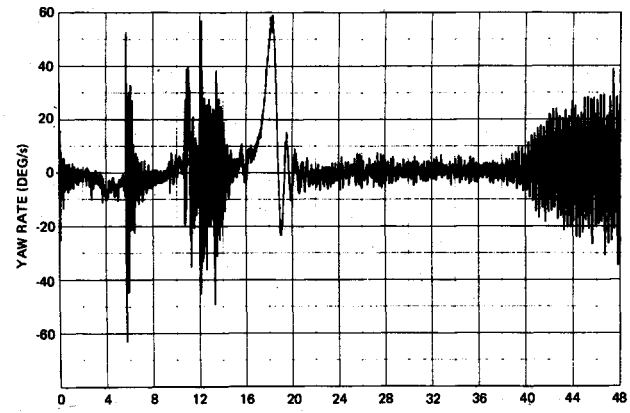

b) Yawing velocity history

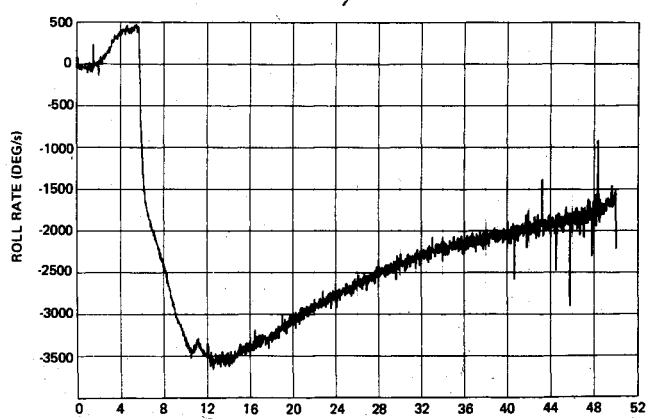

c) Rolling velocity history

Fig. 7 Components of body angular rate determined from onboard rate gyro (time given in sec).

Fig. 7. At payload separation the spin rate was −3550 deg/sec and decreased to approximately −1750 deg/sec, at which time parachute deployment occurred. Aerothermodynamic data[10] indicated that surface recession was great enough to expose the tape edges at payload separation. Heat shield roll torque was therefore operational.

A divergence to approximately 80 deg/sec pitch and 60 deg/sec yaw rate at $T=18.0$ sec is attributed to a momentary roll resonance condition. Passage through resonance was nominal and subsequent damping of the angular rate amplitudes indicates good static and dynamic stability. Achievement of clean payload separation represents a greatly improved capability for this system.

Recovered Vehicle

Nominal performance of the parachute system permitted postflight recovery of the vehicle intact. The thermal shield had considerable delamination along its length. Upon close examination of the shield, no obvious surface discontinuities were detected with any degree of regularity. Some laps were observed, and in some cases the fabric stitching was detected. In addition to these protuberances, some holes were detected in the shield. However, no conclusive evidence in favor of any type of roll-producing surface was obtained.

The recovered nosetip, shown in Fig. 8 with the preflight shape, achieved a turbulent heating profile with severe shoulder erosion at angles 30 to 60 deg from the stagnation point. Stagnation point recession of 0.080 in. was measured, whereas at the sidewall less than 0.005 in. was observed near the base of the tip.

Aerodynamic Analysis

Theoretical Rolling Moment Coefficient

Several models for explaining the observed flight performance have been formulated. Larmour[1] developed a statistical model based upon a large number of flight tests of a low bluntness re-entry configuration; an analytical model[2] based upon cone surface pressure provided favorable agreement with these data. Hull,[12] Wells,[13] Wilson,[14] and Hall[15] have developed theoretical models based upon the individual tape ends, whereas Schurmann[16] has presented a model based upon an experimentally determined "surface" torque coefficient. Three of the models[13-15] are similar, in that surface irregularities associated with the tape seams are postulated to be responsible for the roll torque; they differ in their assumptions regarding the nature of these surface perturbations and the fluid dynamic forces associated with them. The model of Schurmann[16] is based upon experimentally determined surface torque coefficients. (Hull[12] has also postulated recently that the roll torque is a heat shield surface induced effect. However, no predictions based upon his model were available for comparison with the present data.)

Wells[13] and Hall[15] assume that with the onset of turbulent flow, ablation of the heat shield results in the formation of small finlets, the dimensions of which are determined by the thickness and lay-up angle of the carbon phenolic tape. Wilson[14] suggests that the aerodynamic heating results in the formation of oblong holes caused by the oxidation of the thread used to sew the tape together.

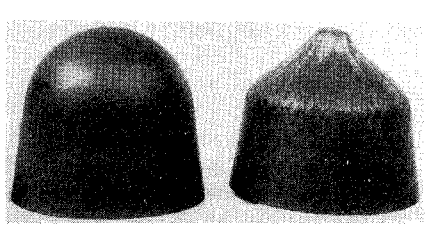

Fig. 8 Comparison of pretest and postflight recovered nosetips showing turbulent erosion pattern.

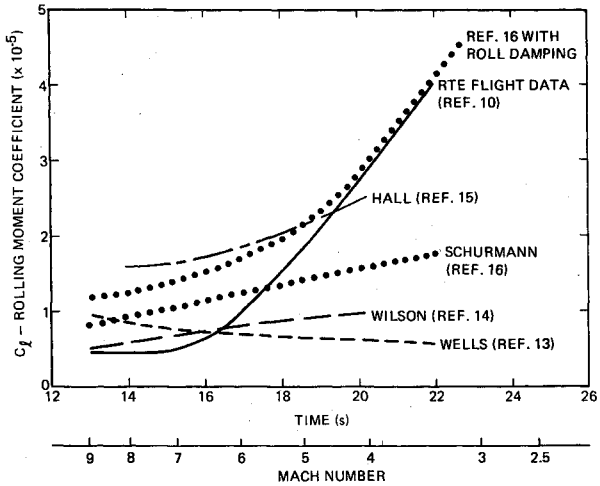

Fig. 9 Comparison of theoretical and flight test rolling moment coefficient.

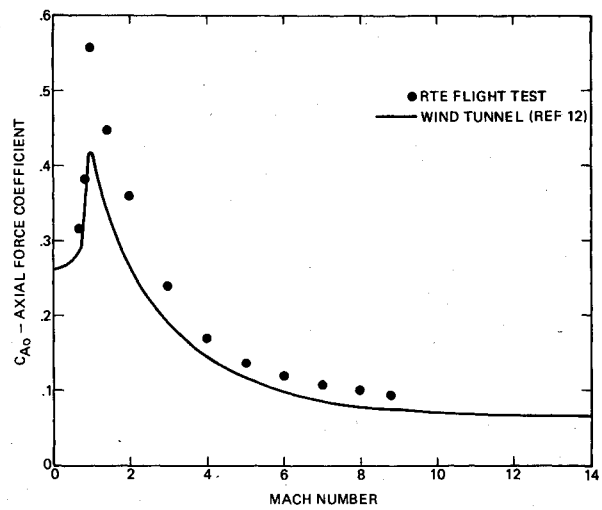

Fig. 10 Axial force coefficient obtained from flight test and wind-tunnel tests.

All of the theories use a "drag coefficient" to determine the aerodynamic forces associated with the surface perturbation: Wells uses for each finlet a coefficient which is characteristic of that obtained for low-speed flow over sheet metal joints; Hall uses a drag coefficient which is selected so that the theoretical and experimental roll torque agree at one specific altitude; Schurmann employs an experimentally determined torque coefficient/unit surface area; and Wilson calculates the drag of a cavity assuming a fully developed cavity vortex flow.

Use of a drag coefficient requires the calculation of an effective dynamic pressure. Wells assumes a 1/7 power velocity profile and constant density and then integrates the momentum flux profile over the height of the finlet. Hall uses a nonsimilar finite-difference boundary-layer code to calculate local flow properties; from these local properties the dynamic pressure is evaluated at the top of the finlet. Schurmann and Wilson use boundary-layer edge dynamic pressure.

After an area, a drag coefficient, and an effective dynamic pressure have been determined, the force acting on the surface perturbation also can be determined, and the total torque on the vehicle can be calculated by integrating over the surface of the vehicle. The results thus obtained are compared with experimental data in the next section.

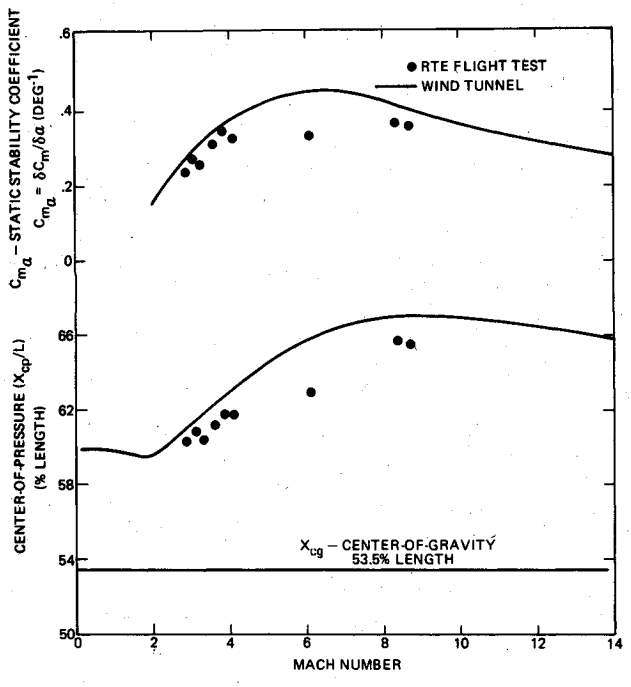

Fig. 11 Comparison of flight test static stability with wind-tunnel data (pitching moment coefficient and center of pressure).

Experimental Rolling Moment Coefficient

To compute the total rolling moment coefficient, the following relation was employed: $C_\ell = 4\dot{p}I_X/Q\pi d^3$. The resulting values are presented in Fig. 9. At Mach 8.8 (the highest Mach number for free flight of the payload) C_ℓ was determined to be 0.44×10^{-5}. The rolling moment coefficient increases significantly with flight time (decreasing Mach number), attaining a value of 7.0×10^{-5} at Mach 2.

A comparison of flight test rolling moment coefficient and theoretical predictions also is shown in Fig. 9. Order-of-magnitude agreement is obtained with each of the theories. At flight times exceeding 16 sec, the flight data indicate a large change in total rolling moment coefficient. With the exception of the calculation of Schurmann, roll damping is not included. Each of the theories tends to overestimate the roll torque for Mach numbers greater than about 6. For $M_\infty < 6$, the prediction of Schurmann, which includes the effect of roll damping, is in excellent agreement with the flight data even down to $M_\infty = 1.5$.

There are two elements that provide some uncertainty in the flight-derived rolling moment coefficient. These are trim-c.g. offset and roll damping effects. The trim angle contribution to roll moment, discussed later, is determined to have a small contribution. The roll damping effect, as indicated by Schurmann,[16] can be especially significant for the present configuration. Wind-tunnel testing[14] at Mach 5 provided roll damping coefficient, C_{ℓ_p}, of -1×10^{-3}. With this value, the roll moment coefficient due to roll damping is determined to be 0.38×10^{-5} at Mach 5 or approximately 25% of the total roll moment coefficient measured at that time. At higher Mach numbers, the roll moment coefficient due to damping, although smaller in magnitude, could be a larger percentage of the total roll coefficient. The roll damping contribution therefore can be significant, especially in light of Schurmann's calculations. Future consideration should be given to this factor if the roll characteristics of TWCP heat shields are to be understood.

Aerodynamic Drag

The axial force coefficient, computed from the onboard axial accelerometers and trajectory parameters, is shown as a function of Mach number in Fig. 10 along with experimentally determined values.[12] The vehicle experienced nearly 20% greater drag than anticipated; this might be attributed to the ablated nosetip shape discussed earlier.

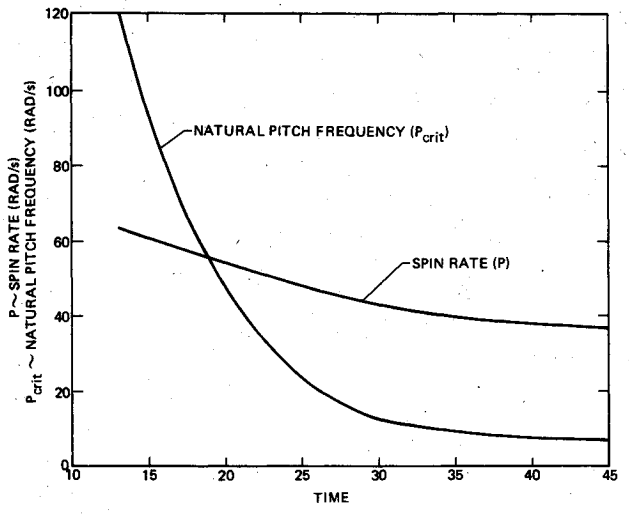

Fig. 12a Spin rate and natural pitch frequency (time given in sec).

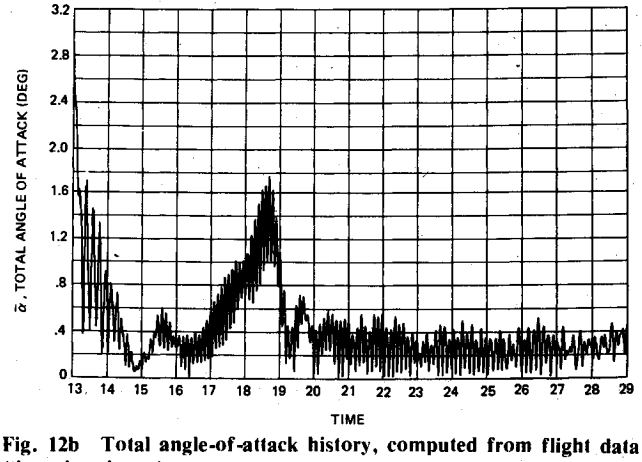

Fig. 12b Total angle-of-attack history, computed from flight data (time given in sec).

Static Stability

An analysis of the lateral motion data produced information on vehicle static stability summarized in Fig. 11 and compared with wind-tunnel data of Ref. 12. A frequency analysis of the lateral motion data indicated less stability than expected. A forward movement of the aerodynamic center of pressure by 1 or 2% at Mach numbers of 3 and 8 and as much as 3% at Mach 6 was determined. This could be a potential problem area for lower static margin vehicles. A possible source of this loss in stability is the shape change in the nosetip. However, additional data would be required to be more conclusive. This shape change also could affect the flowfield over the cone afterbody, which, in turn, would change the roll moment produced by the tape ends.

Using the static stability coefficient C_{M_α} and the dynamic pressure history, the natural pitch frequency was computed; it is presented along with the roll rate history in Fig. 12. Roll resonance is seen to have occurred at about $T=18$ sec. Calculation of the vehicle total angle of attack[10] from flight data indicates that, after damping from an initial disturbance of 3.0 deg due to separation, a divergence to about 1.9 deg at roll resonance was experienced. Resonance amplification was only momentary and the angle of attack subsequently damped to a rolling trim angle with an amplitude of approximately 0.20 deg later in the flight.

Since the vehicle was designed with small out-of-plane mass asymmetry (less than 0.001 in. of c. g. offset), the combination of trim and c.g. offset had a relatively minor effect on the rolling performance of the vehicle. Peak amplification occurs at approximately $T = 18.5$ sec and would result in a roll moment coefficient of approximately 20% of the total measured if the c.g. offset were normal to the trim plane. For those periods during which the trim is not amplified because of resonance, the trim contribution to rolling moment is reduced significantly. For example, at higher Mach numbers ($T \leq 16$ sec) the trim-c.g. offset effect is about 10% of the total in the worst case.

Conclusions

From the results of the roll torque evaluation (RTE) flight test analysis, the following conclusions can be made:

1) A flight test system was developed which provided a controlled experiment for the evaluation of tape-wrapped carbon phenolic (TWCP) heat shield roll torques. The system was highly instrumented, flown in an ablating environment simulating full-scale re-entry, and recovered intact.

2) Good quality telemetry data were obtained on the test vehicle aerodynamic performance and thermal response. Heat shield rolling moment coefficients, computed from the flight data through the Mach range of 2 to 8.8, were significant. Comparisons of flight data with theoretical estimates indicate order-of-magnitude agreement. However, the roll damping on the flight and its relation to the total rolling moment is significant and presents a modeling unknown. An expanded program would be required to be more conclusive. Thermal instrumentation indicated that enough heat shield ablation took place prior to payload separation to expose the aerodynamic surfaces at the tape joints completely.

3) Aerodynamic analysis of the flight data indicated that the vehicle exhibited more drag (approximately 20%) and less static stability (1 to 3% forward movement of the aerodynamic center of pressure) than expected. The source of this anomaly is considered to be the ablated nosetip shape change. The erosion profile suggests that transition occurred near the stagnation point.

Acknowledgment

This work was supported by the U.S. Energy Research and Development Administration. The authors would like to express their appreciation to D. Hall, L. Hull, E. Schurmann, P. Wells, and G. Wilson for helpful discussions and for performing the theoretical calculations with which the present flight data were compared.

References

[1] Larmour, R., "Heatshield Tape Lap Effects on Roll Rate Performance," *Proceedings of the Symposium on Ballistic Re-Entry Vehicle Roll Control,* Aerospace Corp. Rept., TOR-0074 (4450-15)-2, Aug. 1973, Chap. 13.

[2] Kryvoruka, J.K. and Bramlette, T.T., "Heatshield Tape Lap Effects on Re-Entry Vehicle Spin Rate," Sandia Laboratories, Livermore, Calif., SLL-73-0277, Aug. 1973.

[3] Nayfeh, A.H. and Wilson, G.G., "Impact Point Dispersion Due to Spin Reversal," *Journal of Spacecraft and Rockets,* Vol. 7, June 1970, pp. 758-759.

[4] Platus, D.H., "A Note on Re-Entry Vehicle Roll Resonance," *AIAA Journal,* Vol. 5, July 1967, pp. 1348-1350.

[5] Murphy, C.J., "Response of an Asymmetric Missile to Spin Varying Through Resonance," AIAA Paper 71-46, New York, Jan. 1971.

[6] Tobak, M., "Hypothesis for the Origin of Cross-Hatching," *AIAA Journal,* Vol. 8, Feb. 1970, pp. 330-334.

Tobak, M., "Hypothesis for the Origin of Cross-Hatching," *AIAA Journal,* Vol. 8, Feb. 1970, pp. 330-334.

[7] McDevitt, J.B., "An Exploratory Study of the Roll Behavior of Ablating Cones," AIAA Paper 70-562, Tullahoma, Tenn., May 1970.

[8] Williams, E.P., "Experimental Studies of Ablation Surface Patterns and Resulting Roll Torques," AIAA Paper 69-180, New York, Jan. 1969.

[9] Larmour, R., Hall, D., and Novak, R., "Tape-Wrapped Carbon Phenolic Roll Torque Effects on Accuracy Improvement of Ballistic Systems," *Proceedings of the AIAA Joint Strategic Sciences Meeting,* San Diego, Calif., June 2-4, 1976.

[10] Kryvoruka, J.K., "Roll Torque Evaluation (RTE) Vehicle Post Flight Test Report," Sandia Laboratories, Livermore, Calif., SAND76-8001, March 1976.

[11] Rollstin, L.R. and Fellerhoff, R.D., "Aeroballistic and Mechanical Design and Development of the Talos-Terrier-Recruit (TATER) Rocket System With Flight Test Results," Sandia Laboratories, Albuquerque, N.M., SAND74-0440, Feb. 1976.

[12] Hull, L., Lockheed Missiles and Space Corporation, Sunnyvale, Calif., Personal Communication; also *Proceedings of Re-Entry Vehicle Aerodynamic Response Meeting,* Kaman Sciences Corp., Jan. 1976.

[13] Wells, P.B. and Prather, D.W., "Surface Induced Roll Torques from TWCP Heat-Shields," Kaman Sciences Corp., Colorado Springs, K-73-678, Nov. 1973.

[14] Wilson, G.G., "Induced Roll Torques Due to Surface Anomalies at the Tape Splices of Ablated Carbon Phenolic," Sandia Laboratories, Albuquerque, N.M., SAND75-0189.

[15] Hall, D., "Roll Torque Modeling," *Re-entry Vehicle Aerodynamic Response Interchange Meeting,* Jan. 8-9, 1976; also Kaman Sciences Corp., K-76-60(R), Feb. 15, 1976.

[16] Schurmann, E., "Heat Shield Rolling Moment Correlation and Prediction," *Re-entry Vehicle Aerodynamic Response Interchange Meeting,* Jan. 8-9, 1976, also Kaman Sciences Corp., K-76-60(R), Feb. 15, 1976.